Attosecond Probing of Vibrational Dynamics with High-Harmonic Generation

Manfred Lein*

Max Planck Institute for the Physics of Complex Systems, Nöthnitzer Straße 38, 01187 Dresden, Germany and Max Planck Institute for Nuclear Physics, Saupfercheckweg 1, 69117 Heidelberg, Germany

(Received 22 July 2004; published 11 February 2005)

The numerical solution of the time-dependent Schrödinger equation for vibrating hydrogen molecules in few-cycle laser pulses shows that high-harmonic generation is sensitive to the laser-induced vibrational motion. More intense harmonics are generated in heavier isotopes, the difference increasing with the harmonic frequency. Analytical theory reveals a dependence of the harmonics on the vibrational autocorrelation function. With the help of a genetic algorithm, the nuclear motion can be reconstructed from the harmonic spectra with sub-fs time resolution.

DOI: 10.1103/PhysRevLett.94.053004 PACS numbers: 42.65.Ky, 33.80.Rv

The laser-based measurement of ultrafast processes in atoms and molecules has recently advanced into the time scale below one femtosecond. One method [1] utilizes attosecond light pulses obtained from high-order harmonic generation (HHG). In this scheme, the attosecond pulse triggers an atomic process which is then probed by a synchronized laser light wave. Another method [2,3] exploits the presence of attosecond electron wave packets during the interaction of an atom or molecule with an intense laser. These wave packets correspond to electrons that recollide with the core after an excursion in the continuum. Information about the system at the time of recollision is encoded in the products of the collision process: in Refs. [2,3], the kinetic-energy release after fragmentation caused by inelastic scattering was measured.

Instead of fragmentation, recollision may also lead to recombination accompanied by the emission of a photon, i.e., HHG [4,5]. This Letter proposes HHG as an alternative approach to the ultrafast measurement of vibrational dynamics. We consider a vibrational wave packet being launched in the event of ionization by an intense laser field. The subsequent dynamics of the molecular ion is correlated in time with the motion of the electronic continuum wave packet. The recombination of a recolliding electron then probes the state of the parent ion. Hence, the time between ionization and recombination is equivalent to the delay time in a pump-probe scheme. As will be explained in detail below, the scheme involving HHG differs from the method of Refs. [2,3] in two important aspects: (i) due to the relation between the harmonic frequency and the return time of the electron, a range of delay times can be studied without changing the laser wavelength; (ii) the emission of harmonics corresponds to a transition from a state that has evolved over time back into the ground state of the molecule, and the harmonic intensity depends on the overlap of the two states. Therefore, the harmonics are sensitive to small changes of the molecular geometry occurring within a fraction of the vibrational period.

The description of the laser-driven correlated electronic and nuclear wave packet dynamics requires a non-Born-Oppenheimer (non-BO) treatment. For the H_2^+ molecular ion and simplified models thereof, such calculations have been carried by several workers [6]. In molecular ions, however, charge resonance enhanced ionization [7] tends to form complicated initial nuclear wave packets at distances much larger than the equilibrium separation. Well confined wave packets around the ground state bond length are created in strong-field ionization of H_2 [8,9]. Non-BO calculations of HHG in one-dimensional H_2 [10] have been carried out previously, but have focused on selection rules rather than ultrafast wave-packet dynamics. Here, we introduce a non-BO model of H_2 with two-dimensional electron dynamics. This allows us to study the influence of the molecular orientation. In order to limit the computational effort, and since we are here not investigating two-electron effects, we employ a single-active-electron approach. Although this method does not provide access to processes [2,3] involving inelastic rescattering, it is well suited to describe single-electron phenomena such as HHG. The orientation θ of the molecule relative to the field is held fixed, since the rotational motion is negligible on the few-cycle time scale ($\sim$10 fs). In our model, the effective velocity-gauge Hamiltonian for the interaction with a linearly polarized laser field $E(t)$ along the x axis reads (atomic units are used throughout)

$$H_{\mathrm{eff}} = -\frac{\partial_R^2}{M} - \frac{1}{2}\nabla_{\mathbf{r}}^2 - iA(t)\frac{\partial}{\partial x} + V_{\mathrm{eff}}(R, \mathbf{r}), \qquad (1)$$

where $A(t) = -\int_{-\infty}^{t} E(t')dt'$, M is the mass of one nucleus, and R, $\mathbf{r}$ are the internuclear distance and the electron coordinate, respectively. The interaction between the active electron and the nuclei is chosen as

$$V_{\mathrm{eff}}(R, \mathbf{r}) = V_{\mathrm{BO}}^{+}(R) - \sum_{j=1,2} \frac{Z(R, |\mathbf{r} - \mathbf{R}_j|)}{\sqrt{|\mathbf{r} - \mathbf{R}_j|^2 + 0.5}}, \qquad (2)$$

where $\mathbf{R}_j$ are the positions of the nuclei. For $|\mathbf{r}| \to \infty$ this function approaches $V_{\mathrm{BO}}^{+}(R)$, the lowest BO potential of H_2^+. This amounts to the assumption that the removal of one electron creates H_2^+ in its electronic ground state. In the soft-core interaction, we have introduced an effective nuclear charge $Z(R, u) = [1 + \exp(-u^2/\sigma^2(R))]/2$, which

mimics the average screening of the nuclei by the second electron: $Z(R,u) \to 1$ for $u \to 0$, and $Z(R,u) \to 1/2$ for $u \to \infty$. The screening parameter $\sigma(R)$ is adjusted such that the resulting lowest BO potential of the neutral model molecule matches the real H_2 BO potential taken from [11]. For the laser field, trapezoidally shaped 6-cycle pulses are chosen. The wave function $\Phi(R, \mathbf{r}, t)$ is represented in Cartesian coordinates, and the time-dependent Schrödinger equation is solved numerically by the split-operator method [12] with 2048 time steps per laser cycle, starting from the ground state of the system. Absorbing boundaries are employed for all coordinates. The spectrum of emitted radiation is calculated by Fourier transforming the time-dependent dipole acceleration [13]. A grid size of $L_x \times L_y = 180 \times 45$ a.u. for the electron and a range of $R = 0.6 \ldots 3.7$ a.u. for the internuclear distance have proven sufficient for converged harmonic spectra.

Figure 1 shows a sample of calculated harmonic spectra for various orientations of H_2 in a 780 nm pulse with intensity 4×10^{14} W/cm^2 (laser frequency $\omega = 0.0584$ a.u., and field amplitude $E_0 = 0.107$ a.u.). The cutoff at the energy $3.17U_p + I_p$ [4,5] is clearly visible in all spectra. Here, $U_p = E_0^2/(4\omega^2)$ is the ponderomotive potential and I_p is the ionization potential.

When θ is not too large, the spectrum exhibits a minimum due to two-center interference as described for clamped nuclei in Refs. [14,15]. Thus, as a first important result, we find that this minimum persists when the vibrational motion is taken into account.

In order to study the influence of vibrations, we move on to a comparison of isotopes. In Fig. 2, we compare the harmonics from the molecules H_2, D_2, and T_2, aligned perpendicular to the field. This orientation is chosen because it does not give rise to a two-center interference pattern. The calculation has been carried out for two laser wavelengths, 780 nm and 1200 nm. In both cases we clearly observe that heavier isotopes generate more intense harmonics. The ratio between the isotopes equals approximately unity when the harmonic order goes to zero. On average, the ratios grow with increasing harmonic order, even though the behavior is nonmonotonic. It is noticeable that the oscillations are most pronounced near the cutoff. For D_2 vs H_2, an average ratio of about 1.5 is reached at the cutoff.

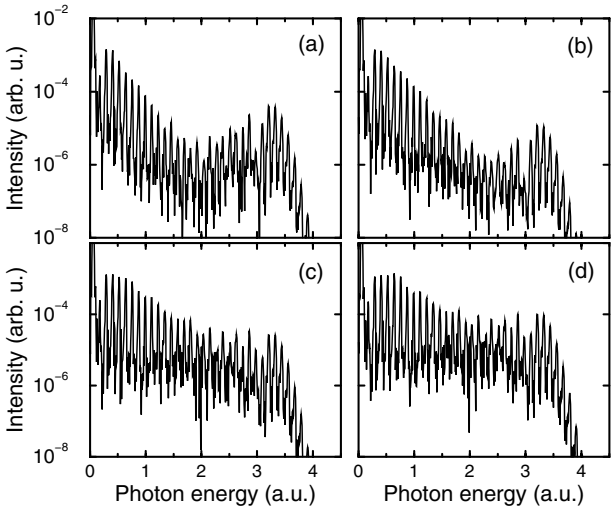

FIG. 1. Calculated harmonic spectra for H_2 in a 780 nm pulse with 4×10^{14} W/cm^2 intensity. The orientation of the molecule with respect to the field is (a) $\theta = 0°$, (b) $\theta = 30°$, (c) $\theta = 60°$, (d) $\theta = 90°$.

Experiments with randomly oriented molecules are much easier realized than with aligned molecules. The theoretical description of a random ensemble, however, requires the calculation of the harmonic intensities and phases for all possible orientations, and these contributions have to be added coherently [16]. This analysis has been carried out for D_2 and H_2 in the 780 nm case, see Fig. 2(a). The resulting ratio is almost identical to the case of perpendicular alignment. The ratio is even slightly enhanced. The similarity arises because the contributions near $\theta = 90^o$ dominate the signal in the random ensemble for two reasons: (a) the contributions are weighted by a geometrical factor $\sin\theta$ [16]; (b) two-center interference is constructive around $\theta = 90^o$ [15]. The isotope effect should therefore be easily measurable in an experiment with a randomly oriented ensemble. Even if the experimental densities of H_2 and D_2 differ from each other, the slope in the harmonic ratio will survive.

The difference between the isotopes indicates that slower vibration leads to more intense harmonics. To investigate this point further, we incorporate the vibrational motion into the Lewenstein model of HHG [17], which was formulated for atoms. We start from the length-gauge Hamiltonian for a laser-driven H_2 molecule with fixed orientation,

$$H = -\frac{\nabla_1^2}{2} - \frac{\nabla_2^2}{2} - \frac{\partial_R^2}{M} + V(\mathbf{r}_1, \mathbf{r}_2, R) + E(t)(x_1 + x_2), \quad (3)$$

where $\mathbf{r}_1$, $\mathbf{r}_2$ are the electron coordinates and V is the sum

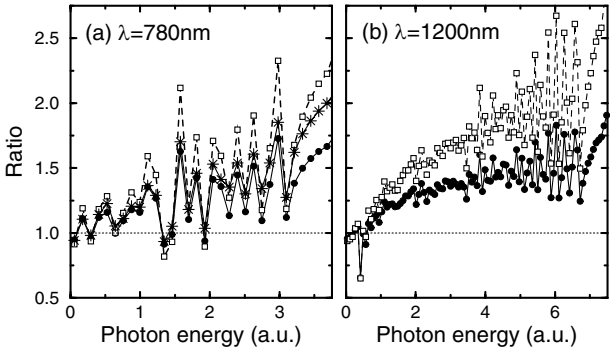

FIG. 2. Ratio between harmonic intensities in different isotopes (aligned perpendicular to the field): D_2 vs H_2 (circles connected by solid lines), T_2 vs H_2 (squares connected by dashed lines). Shown are the ratios for odd harmonics at 780 nm wavelength [panel (a)] and 1200 nm wavelength [panel (b)]. Panel (a) includes also the ratio D_2 vs H_2 for randomly oriented molecules (stars). The laser intensity is 4×10^{14} W/cm^2.

of the Coulomb interactions between all particles. Following Ref. [17], we assume that (a) no bound states other than the BO ground state are populated, (b) the depletion of the ground state can be neglected, and (c) while in the continuum, the active electron does not interact with the core. Additionally, we assume that only a single electron can become active; i.e., if one of the electrons has been excited into the continuum, the second electron will not couple to the field and will always remain in the lowest BO state of the molecular ion.

We can then expand the full wave function as

$$\Psi(\mathbf{r}_1, \mathbf{r}_2, R, t) = e^{-iE_0 t}\Big\{\Psi_0 + \int \frac{d^3k}{(2\pi)^3}\,\phi(\mathbf{k}, R, t) \times [e^{i\mathbf{k}\cdot\mathbf{r}_1}\psi_R^+(\mathbf{r}_2) + e^{i\mathbf{k}\cdot\mathbf{r}_2}\psi_R^+(\mathbf{r}_1)]\Big\}, \quad (4)$$

where $\Psi_0 = \chi_0(R)\psi_R(\mathbf{r}_1, \mathbf{r}_2)$ is the real-valued ground-state wave function of H_2 (or its isotopes) in the BO approximation, E_0 is the ground-state energy, and $\psi_R^+(\mathbf{r})$ is the electronic ground-state BO wave function of H_2^+. Neglecting the non-BO couplings and laser-field interaction for ψ_R^+, the time-dependent Schrödinger equation $i\partial\Psi/\partial t = H\Psi$ is transformed to

$$\dot{\phi}(\mathbf{k}, R, t) = -i\left[\frac{\mathbf{k}^2}{2} - \frac{\partial_R^2}{M} + V_{\mathrm{BO}}^+(R) - E_0\right]\phi(\mathbf{k}, R, t) + E(t)\frac{\partial\phi(\mathbf{k}, R, t)}{\partial k_x} - iE(t)d_x(\mathbf{k}, R)\chi_0(R), \quad (5)$$

where $d_x(\mathbf{k}, R) = \int d^3r_1 d^3r_2 e^{-i\mathbf{k}\cdot\mathbf{r}_1}\psi_R^+(\mathbf{r}_2)x_1\psi_R(\mathbf{r}_1, \mathbf{r}_2)$ is the bound-free dipole matrix element. By taking

$$d_x(\mathbf{k}, R)\chi_0(R) \approx \bar{d}_x(\mathbf{k})\chi(R, 0) \quad (6)$$

we make the assumption that ionization launches a vibrational wave packet $\chi(R, 0)$ that is uncorrelated with the initial momentum $\mathbf{k}$ of the outgoing electron. Under the initial condition $\phi(\mathbf{k}, R, 0) = 0$, the solution of Eq. (5) is

$$\phi(\mathbf{k}, R, t) = -i\int_0^t dt' E(t')\bar{d}_x(\mathbf{k} - \mathbf{A}(t) + \mathbf{A}(t'))\chi(R, t - t') \times e^{-i\int_{t'}^t dt''\{[\mathbf{k}-\mathbf{A}(t)+\mathbf{A}(t'')]^2/2 - E_0\}} \quad (7)$$

with $\mathbf{A}(t) = (A(t), 0, 0)$. The vibrational wave packet $\chi(R, \tau)$ obeys the Schrödinger equation

$$i\frac{\partial\chi(R, \tau)}{\partial\tau} = \left[-\frac{\partial_R^2}{M} + V_{\mathrm{BO}}^+(R)\right]\chi(R, \tau). \quad (8)$$

Neglecting continuum-continuum transitions, the time-dependent dipole moment along x, $D_x(t) = -\langle\Psi(t)|x_1 + x_2|\Psi(t)\rangle$, is

$$D_x(t) = -2\int \frac{d^3k dR}{(2\pi)^3} d_x^*(\mathbf{k}, R)\chi_0(R)\phi(\mathbf{k}, R, t) + \text{c.c.} \quad (9)$$

In this last equation, the use of approximation (6) is questionable because the range of possible values for $\mathbf{k}$ and R is large, and interference effects give rise to a strong dependence of the matrix element on the projection of the internuclear distance on the field axis [15]. Nevertheless the approximation is reasonable in the case of perpendicular alignment where the two-center interference is constructive independently of R. This leads to

$$D_x(t) = 2i\int_0^t dt' E(t')C(t - t')\int \frac{d^3p}{(2\pi)^3}\bar{d}_x^*[\mathbf{p} + \mathbf{A}(t)] \times \bar{d}_x(\mathbf{p} + \mathbf{A}(t'))e^{-i\int_{t'}^t dt''\{[\mathbf{p}+\mathbf{A}(t'')]^2/2 - E_0\}} + \text{c.c.}, \quad (10)$$

where

$$C(\tau) = \int dR\chi^*(R, 0)\chi(R, \tau) \quad (11)$$

is the vibrational autocorrelation function. Physically, $\tau = t - t'$ is the travel time between ionization and recombination. Equation (10) is essentially identical to the Lewenstein model except for the appearance of $C(\tau)$. The intensity of a harmonic that is dominated by a single value of τ is therefore proportional to $|C(\tau)|^2$.

Figure 2 is easily interpreted in terms of the autocorrelation function. The vibrational motion is faster in the lighter isotope and therefore, $C(\tau)$ decreases more rapidly away from its initial value, leading to weaker harmonics. Although in principle many different travel times contribute to one harmonic, long travel times have only little weight due the spreading of the electron wave packet. If only the shortest trajectory is taken into account, we have a one-to-one mapping between travel time and harmonic frequency, with larger times producing higher frequencies (see Fig. 1 of Ref. [17]). Thus the difference between isotopes grows with increasing frequency as the dominant travel time increases. For harmonic frequencies close to the cutoff, HHG is dominated by a pair of nearly equal travel times. The interference between the two amplitudes is known to produce a pattern of minima and maxima in the spectrum. Figure 2 shows that a similar pattern appears in the ratio between isotopes.

For the case of longer pulses not considered here, the weight of later returns may be substantial due to maxima in the autocorrelation function related to the vibrational period. With few-cycle pulses this possibility is excluded.

To extract dynamical information from the harmonic spectra, we first map the photon energies to the travel time using the semiclassical model of Ref. [4]: by ionization, a classical free electron appears with zero velocity at the origin, is accelerated by the time-dependent field, and finally revisits the core with return energy E_r. Recombination generates a photon with energy $\hbar\Omega = E_r + I_p$. Including only short trajectories ($\omega\tau < 4.09$ a.u.), the travel time as a function of the return energy is fitted as

$$\omega\tau = 0.786[f(E_r/U_p)]^{1.207} + 3.304[f(E_r/U_p)]^{0.492} \quad (12)$$

with $f(x) = \arccos(1 - x/1.5866)/\pi$. The result of the analysis is shown in Fig. 3(a) for D_2/H_2 in the 1200 nm

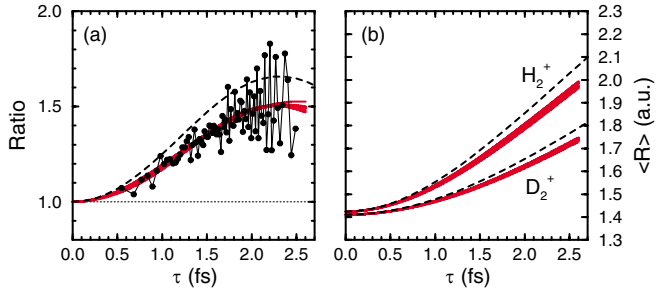

FIG. 3 (color online). (a) Data points show the ratio between harmonics in D_2 and H_2 versus electron travel time for a 1200 nm laser pulse. Smooth lines are the autocorrelation ratio calculated from the vibrational wave-packet dynamics in potentials from the reconstruction procedure (solid, red) or in the exact H_2^+ BO potential (dashed line). (b) Time evolution of the internuclear distance, as reconstructed from the D_2/H_2 harmonic spectra (solid, red) and time evolution in the exact potential (dashed lines).

case. For comparison, we solve the vibrational Schrödinger equation, Eq. (8), numerically with the initial condition $\chi(R, t = 0) = \chi_0(R)$, and evaluate the autocorrelation function, Eq. (11), for H_2^+ and D_2^+. The figure shows that the resulting autocorrelation ratio $|C^{D_2^+}(\tau)/C^{H_2^+}(\tau)|^2$ predicts the correct trend, but slightly overestimates the ratio of harmonic intensities. To reconstruct the vibrational dynamics from the spectra of D_2 and H_2, we first note that the ratio of harmonics appears to approach unity as $\tau \to 0$. With Eq. (11), this means that the initial wave packets $\chi(R, 0)$ in H_2 and D_2 have approximately the same norm. Excluding the unlikely accident that this is achieved by a special R dependence of the dipole matrix element, it shows that $\chi(R, 0) \approx \chi_0(R)$. Knowing the initial state, we adapt a genetic algorithm (GA) [18] to optimize an ionic BO potential such that the calculated wave-packet motion (obtained by solving the 1D vibrational Schrödinger equation) minimizes the sum of squared deviations of the autocorrelation ratio from the ratio of harmonics. The potential is parametrized as

$$V^+(R) = \frac{1}{R} - \frac{1}{2} + \frac{\alpha_1}{(\alpha_2 + R)} + \frac{\alpha_3}{(\alpha_4 + R^2)} + \alpha_5 \exp(-\alpha_6 R) + \alpha_7 \exp(-\alpha_8 R^2). \quad (13)$$

Here, we have used the known limits $V^+(R) \simeq 1/R$, $R \to 0$ and $V^+(R) \to -0.5$ a.u., $R \to \infty$ to impose restrictions on the potential. We furthermore enforce $V^+(R) \simeq 2 + 1/R$ for $R \to 0$ by eliminating one parameter, and we discard potentials that do not give initially repulsive wave-packet motion. The GA is iterated 1000 times with a population size of 40 individuals. The results depend only slightly on the GA parameters. For numerous runs, the obtained time evolution of the expectation value of the internuclear distance in H_2^+/D_2^+ is shown in Fig. 3(b). The result is quite similar to the propagation in the exact BO potential; see the dashed curves in Fig. 3(b). The corresponding autocorrelation ratios fit the harmonic ratios perfectly, as can be seen in Fig. 3(a). The small deviations with respect to the exact potential arise because $\chi(R, 0) = \chi_0(R)$ is not strictly fulfilled. We conclude that if a small number of reasonable assumptions are made, the nuclear wave-packet motion can be reconstructed with attosecond time resolution. In the experiment of Ref. [2], the laser wavelength was varied to measure the ionic state for various delay times. The present scheme gives access to different delay times without changing the wavelength, simply by observing different harmonic orders.

In summary, HHG in molecules depends on the isotope and gives temporal information about the vibrational dynamics. The harmonics measure approximately the vibrational autocorrelation function of the molecular ion with attosecond resolution. We have demonstrated a scheme to reconstruct the nuclear motion from measurable spectra and have therefore presented an alternative approach to measurements on the attosecond time scale.

*Electronic address: manfred.lein@mpi-hd.mpg.de

[1] R. Kienberger *et al.*, Nature (London) **427**, 817 (2004).
[2] H. Niikura *et al.*, Nature (London) **417**, 917 (2002); H. Niikura *et al.*, Nature (London) **421**, 826 (2003).
[3] A. S. Alnaser *et al.*, Phys. Rev. Lett. **91**, 163002 (2003).
[4] P. B. Corkum, Phys. Rev. Lett. **71**, 1994 (1993).
[5] K. C. Kulander, J. Cooper, and K. J. Schafer, Phys. Rev. A **51**, 561 (1995).
[6] S. Chelkowski, T. Zuo, O. Atabek, and A. D. Bandrauk, Phys. Rev. A **52**, 2977 (1995); K. C. Kulander, F. H. Mies, and K. J. Schafer, *ibid.* **53**, 2562 (1996); S. Chelkowski, C. Foisy, and A. D. Bandrauk, *ibid.* **57**, 1176 (1998); W. Qu, Z. Chen, Z. Xu, and C. H. Keitel, *ibid.* **65**, 013402 (2001); B. Feuerstein and U. Thumm, *ibid.* **67**, 063408 (2003).
[7] T. Seideman, M. Y. Ivanov, and P. B. Corkum, Phys. Rev. Lett. **75**, 2819 (1995); T. Zuo and A. D. Bandrauk, Phys. Rev. A **52**, R2511 (1995).
[8] X. Urbain *et al.*, Phys. Rev. Lett. **92**, 163004 (2004).
[9] M. Lein, T. Kreibich, E. K. U. Gross, and V. Engel, Phys. Rev. A **65**, 033403 (2002).
[10] T. Kreibich, M. Lein, V. Engel, and E. K. U. Gross, Phys. Rev. Lett. **87**, 103901 (2001).
[11] W. Kołos, K. Szalewicz, and H. J. Monkhorst, J. Chem. Phys. **84**, 3278 (1986).
[12] M. D. Feit, J. A. Fleck, Jr., and A. Steiger, J. Comput. Phys. **47**, 412 (1982).
[13] K. Burnett, V. C. Reed, J. Cooper, and P. L. Knight, Phys. Rev. A **45**, 3347 (1992).
[14] M. Lein, N. Hay, R. Velotta, J. P. Marangos, and P. L. Knight, Phys. Rev. Lett. **88**, 183903 (2002).
[15] M. Lein, N. Hay, R. Velotta, J. P. Marangos, and P. L. Knight Phys. Rev. A **66**, 023805 (2002).
[16] M. Lein *et al.*, J. Mod. Opt. **52**, 465 (2005).
[17] M. Lewenstein, P. Balcou, M. Y. Ivanov, A. L'Huillier, and P. B. Corkum, Phys. Rev. A **49**, 2117 (1994).
[18] D. L. Carroll, http://cuaerospace.com/carroll/ga.html.